

Hybrid E.M. modes inside a hollow metallic circular guide  
with dielectric coating, Vector Potential Method

Application to photonics and THz acceleration of particles

Jean-Luc BABIGEON

8 septembre 2022

# Table des matières

|          |   |           |
|----------|---|-----------|
| <b>1</b> | <b>ACCELERATING FIELDS INSIDE A GUIDE - GENERIC</b>                             | <b>4</b>  |
| <b>2</b> | <b>HYBRID MODES INSIDE A CYLINDRICAL COATED GUIDE</b>                           | <b>6</b>  |
| 2.1      | Classification of hybrid HE/EH modes . . . . .                                  | 6         |
| 2.2      | Topology of modal space and basis completion . . . . .                          | 8         |
| 2.3      | Basis of VPM . . . . .  | 9         |
| <b>3</b> | <b>CODE DESCRIPTION</b>   | <b>11</b> |
| 3.1      | General . . . . .   | 11        |
| 3.2      | Preparation and conditioning of the input parameters . . . . .                  | 12        |
| 3.3      | Building the matrix and solving for longitudinal propagation constant . . . . . | 13        |
| 3.4      | Calculation of C coefficients . . . . .   | 14        |
| 3.5      | Calculation of scalar potentials and electromagnetic components . . . . .       | 15        |
| <b>4</b> | <b>DISCUSSION</b>   | <b>17</b> |
| 4.1      | Use of different Special Functions among publications . . . . .                 | 17        |
| 4.2      | Various divergences to [26] . . . . .   | 18        |
| <b>5</b> | <b>RESULTS</b>  | <b>19</b> |
| 5.1      | Characteristic curve $kz = f(a/b)$ for different ratios $a/b$ . . . . .         | 19        |
| 5.1.1    | Numerical method . . . . .  | 19        |
| 5.1.2    | Help to user : guess of approximate $kz=f(a/b)$ curve . . . . .                 | 22        |
| 5.1.3    | Analytical method . . . . .   | 27        |
| 5.2      | Dispersion curves . . . . .   | 28        |
| 5.3      | Computation of electromagnetic fields and potentials . . . . .                  | 29        |
| 5.3.1    | Lossless example, dielectric rod guide at 1GHz . . . . .                        | 29        |
| 5.3.2    | Bounded guide, example in THz region . . . . .                                  | 34        |
| <b>6</b> | <b>PERSPECTIVES</b>   | <b>35</b> |
| 6.1      | Elliptical guides . . . . .   | 35        |
| 6.2      | Losses . . . . .  | 35        |
| 6.3      | Magnetic materials . . . . .  | 35        |
| 6.4      | Multi-layer extension . . . . .   | 35        |
| 6.5      | Frequency dependant permittivity . . . . .                                      | 35        |
| <b>7</b> | <b>CONCLUSION</b>   | <b>36</b> |
|          | <b>Annexe</b>   | <b>37</b> |
| .1       | Solutions E,H in cylindrical coordinates . . . . .                              | 38        |
| .2       | The guide is finite/infinite . . . . .  | 39        |
| .3       | Derivation of the superposition coefficients . . . . .                          | 39        |
| .4       | Resolution of the homogeneous system . . . . .                                  | 40        |

## Table des figures

|    |  |    |
|----|--|----|
| 1  | Proposal of modal space . . . . .  | 9  |
| 2  | Actual version of code HMC ver 1.0 . . . . .   | 11 |
| 3  | Graph of $kz$ versus $a/b$ . . . . .   | 12 |
| 4  | Principle of Muller method, after [26] . . . . .   | 15 |
| 5  | Slice of $E_\rho$ , $b=0.012m$ , $a=0.5*b$ , rod of $\epsilon_1 = 37.6, \epsilon_2 = 1.0, f = 3GHz$ . . . . .        | 16 |
| 6  | Harrington reference for HE11 . . . . .  | 20 |
| 7  | First calculation of HE11 mode with $a/b$ variable . . . . .   | 20 |
| 8  | Optimised simulation, with representation of the first guess curves . . . . .  | 20 |
| 9  | Real and imaginary parts of TE11 and TM11 modes[26] . . . . .  | 24 |
| 10 | Real and imaginary parts of TE11 and TM11 modes, inversion of indexes . . . . .                                      | 25 |
| 11 | Low losses with $b = 0.5in, \epsilon_1 = 37.6 - 0.01j, \frac{a}{b} = 0.3646, 4GHz$ [26] . . . . .                    | 26 |
| 12 | High losses with $b = 0.6916in, \epsilon_1 = 23.9 - 15.296j, a = 0.5008in, 4GHz$ [26] . . . . .                      | 26 |
| 13 | Scan of $kz$ values at a fixed frequency . . . . .   | 30 |
| 14 | Frequency 1GHz, $b = 0.4\lambda, \epsilon_1 = 10, \epsilon_2 = 1, \mu_1 = \mu_2 = 1, a = 0.1b$ . . . . .             | 31 |
| 15 | $a = 0.2b$ . . . . .   | 31 |
| 16 | $a = 0.3b$ . . . . .   | 31 |
| 17 | $a = 0.4b$ . . . . .   | 31 |
| 18 | Frequency 1GHz, $b = 0.4\lambda, \epsilon_1 = 10, \epsilon_2 = 1, \mu_1 = \mu_2 = 1, a = 0.1b$ . . . . .             | 32 |
| 19 | $a = 0.2b$ . . . . .   | 32 |
| 20 | $a = 0.3b$ . . . . .   | 32 |
| 21 | $a = 0.4b$ . . . . .   | 32 |
| 22 | Frequency 1GHz, $b = 0.4\lambda, \epsilon_1 = 10, \epsilon_2 = 1, \mu_1 = \mu_2 = 1, a = 0.4b$ . . . . .             | 33 |
| 23 | Frequency 1GHz, $b = 0.4\lambda, \epsilon_1 = 10, \epsilon_2 = 1, \mu_1 = \mu_2 = 1, a = 0.4b$ . . . . .             | 33 |
| 24 | $E_{rho}$ , HE mode, fiber $b = 0.4\lambda, f = 300GHz$ , rod 0.6mm, $\epsilon_1 = 37.6, \epsilon_2 = 1.0$ . . . . . | 34 |

# 1 ACCELERATING FIELDS INSIDE A GUIDE - GENERIC

Future generations of colliders are a hot speculating subject, due to high costs of standard techniques. It becomes now clear that projects of klystron and standard electron optics for HEP colliders are cumbersome, not enough performing for High Energy Physics objectives, and above all budgets of our present world.

Among new acceleration techniques, oriented to compacity, are laser plasma and -with relatively low cost machines- dielectric acceleration. Last technique subdivides into THz modes-smaller copy of standard above techniques- and photonics, for instance « on-chip accelerator »<sup>[2]</sup>.

For these last acceleration schemes and non conventional techniques, we need to better know the behaviour of electromagnetic fields inside guides. We can mention such guides like photonic gap, rectangular strip lines and circular dielectric guides with metallic sheath (metallized fiber).

Metallized dielectric fibers are planned to be used for some THz schemes, although their advantage is not so clear for photonics. Indeed, a skilled combination of indexes in optical fibers, could permit to skip the use of metallic sheet, by naturally mismatching the radial infinite component of fields.

The present study deals with the description and the analytical simulation of electromagnetic fields and of their modes inside a dielectric multi layers dielectric fiber covered with metallic sheet<sup>1</sup>. It presents also the first draft of a simulation code, which is a translation of an existing fortran code; the principle of the code, and theoretical foundations, have been also described in the Master Thesis in reference <sup>[26]</sup>.

Of course we could have re-used that code as-is, since fortran compilers are yet active for PCs, but the version was only a part of several codes -non documented- and it was estimated more efficient to develop a similar code with a real friendly interface (which was not the case) and modern languages. Incidentally some unclear points were found in the original text of the Thesis and inside the associated fortran code, so it was an additional reason for starting from scratch.

Our choice has been oriented to Debian linux machines, with open source codes; the code is implemented in a local mode; all the tools are exportable easily in a notebook way, like Jupyter notebook.

A gnome-like interface based on Gtk+ widgets is to be implemented.

For the computation, I use Julia language <sup>[8]</sup><sup>2</sup>, which may be chained with the Gtk interface.

---

<sup>1</sup>in all the following, named multilayered dielectric fiber

<sup>2</sup>Julia has many advantages over tools like Matlab, for instance a very fast compiler, near the speed of C/C++ compilers

That publication presents the following chapters :

1. recalls of theoretical basis of electromagnetic modes inside a multi-layer dielectric fiber,
2. description of the code
3. a few illustrative examples

As many points are detailed in [26], some recalls are added for that code comprehension, and some items are found in it, obscure or somehow inexact, inviting the reader to report to that reference if necessary.

The « Eigen Mode » is provided by many softwares, like OpenEMS[11]. Benchmarking with commercial codes should be planned during/as soon as the code reaches a stable status.

## 2 HYBRID MODES INSIDE A CYLINDRICAL COATED GUIDE

Among numerous references, Harrington [4] describes hybrid electromagnetic modes. Indeed, if we let propagate electromagnetic energy inside a void guide (with no dielectric inside, but only vacuum/air), the elementary quantified solutions are TE and TM modes, which are not coupled. A TE mode, which has only a longitudinal magnetic component, can exist by itself without any other TM contribution, and conversely, it is theoretically possible to induce electric acceleration, for instance with a pure TM01 mode.

The situation is not as trivial if circular dielectric layer(s) are inserted inside the geometry. Instead observing pure TE/TM modes, we notice a combination of these, particularly a mixture of magnetic and electric longitudinal components. Their conventional notation becomes HExy or EHxy, depending on whether E or H component is predominant, and they constitute a -non complete but degenerate- basis in vectored sense[12]. EM Mode analysis have of course a major importance for acceleration designs, while the Thesis in reference manifests no interest in acceleration, only in study of propagation and losses of the transverses modes. Indeed, its original application was the evaluation of mode attenuation by feedthroughs of shielded enclosure. It explains why no  $E_z$  or  $H_z$  result was reported in the original program.

Last of all, if we are interested by polarised fields, we may prefer the LPmn basis [14]. LPmn, asymptotic of HE/EH, are allowed to radiate in space, due to absence of external metallic wall, which implies that limit conditions are different. Moreover, LPmn is an approximate basis due to coarse hypothesis of potentials and field continuity across interfaces, adapted to low contrasts permittivities, and having degeneracies. Hybrid HE/EH take better into account the details of accelerating and deflecting fields of electron optics.

### 2.1 Classification of hybrid HE/EH modes

As that part will superpose a very studied question, it will be only summarised. As we should like to create a basis, similarly as pure basis TE/TM, the following tentatives were done in the past, to distinguish HE and EH modes, and to enumerate them :

1. to compare the relative amplitude of  $E_z$  viz  $H_z$ ,
2. to quantify it by a factor of merit, [17], [9]
3. to identify a HE,resp EH mode by its asymptotic TE, resp TM companion for -nearly- homogeneous guide,[26]
4. to add some low losses amount and to break degeneracy's around cutoff frequency [26]

The first method is far too qualitative, does not bring a reliable classification, and necessitates an *a-priori* numerical knowledge of z-field components. The second method

is well adapted to dielectric systems like optical fibers, but does not apply to every configurations. Last both methods may be combined and to define  $HE/EH_{mn}$ . Relative to (non-linear and) anisotropic materials, [16], only first criterion, allied to study of power loss has been possible, and HE/EH indexes mn may not be defined.

Let's take a hollow cylindrical metallic guide of internal void radius a, suppose it oversized ( $a \gg \lambda$ ), and recall properties of cylindrical TE,TM modes [22] :

|                               |                  |                 |                 |                  |
|-------------------------------|------------------|-----------------|-----------------|------------------|
| $TE_{mn}(J'n(\tau_{mn}) = 0)$ | $TE_{11}(1.841)$ | $TE_{01}(3.83)$ | $TE_{12}(5.33)$ | $TE_{02}(7.016)$ |
| $TM_{mn}(Jn(\tau_{mn}) = 0)$  | $TM_{01}(2.405)$ | $TM_{11}(3.83)$ | $TM_{02}(5.52)$ | $TM_{12}(7.016)$ |

The cutoff frequency being  $f_c = \frac{c\tau_{mn}}{2\pi a}$ , where  $\tau_{mn}$  is either the zero of the Bessel or its derivative, the modes have been ordered in growing frequency occurrence. One guesses that excitation at  $frequency \propto 3.83$  should hybridise easily  $TE_{12}$  and  $TM_{02}$ . We could call hybrid child,  $HE_{12}$  or  $EH_{02}$ <sup>3</sup>. Moreover, the frequency criteria is enforced by a similar azimuthal distribution. But also, generally, the experimental excitations are not pure CW, their bandwidth may cover the frequencies 1.841 and 2.405. It is known that due to losses of high orders, lowest order modes are leaders. So the « deflecting mode »  $HE_{11}$  (or  $EH_{01}$  ?) will often occur.

But there is no gold rule to forbid a coupling between  $TE_{11}$  and  $TM_{12}$  ( $HE_{11}$ ,  $EH_{12}$ )! We just assume that  $EH_{12}$ 's amplitude will be low relatively to the precedent ones. Note that it is necessary to enumerate both HE and EH modes to come back bijectively to pure TE/TM components. Finally we don't exclude triplet or higher hybridisation, for instance in adiabatic phases of transient configurations, but in practice, the N-bodies systems fall in attractive basins of more stable 2-bodies.

It is deduced that  $HE/EH_{mn}$  family denomination concept, based on the corresponding name of the asymptotic companion, is today pertinent at least for linear inhomogeneous dielectric or magnetic guides with step or graded indexes, in optical fibres and hollow clad metallic guides, and we experimented last methods for their classification. It is expected that it may be extended to frequency dependant permittivities, provided that they are isotropic and linear, which is an important case for THz or dielectric acceleration of particles. An extension of that convention to gyromagnetic materials with tensor permittivities, seems to be successful [25]. Our corresponding code is to be updated for taking account frequency dependant permittivities, soon.

---

<sup>3</sup>the standard denomination is however  $TE_{11}, TM_{11} \rightarrow HE/EH_{11}$

## 2.2 Topology of modal space and basis completion

Here are placed some out-of-concern ideas, generated by the present study. Being inserted in the Introduction, they have no implication and that part may be skipped.

There are several concepts around topological states, linking the Maxwell equations with Dirac one, [5], and applied to cylindrical geometries showing equivalence with bounded Jackiw-Rebbi states. They all rely on Index Theorem, ie searching topological invariant linked with the (eigen) modes.

Here, we analyse rather the continuous transition between « pure modes » and hybrid one, and it suggests to consider them as immersed in the topological hypersurface structure of a differential manifold, [18] which we denote by « modal manifold ». Firstly, we exploit the interesting remark from Hahn [3]. starting from the (complex) vector dispersion law :  $k_i^2 = k_z^2 + k_\rho^2$ , (i, index of the medium), we see that in the neighbourhood of cutoff,  $k_i \sim k_z$ , so the mode has its wave vector nearly parallel with propagation direction. Inversely, at high frequencies asymptote,  $k_i \sim k_\rho$ , and pure TE/TM modes behave as quasi-TEM waves. Moreover, they become degenerate, which we show later in the dispersion curves of  $HE_{11}$  mode.

Now let's try to build on a proper differential manifold structure. We need to define a congruence, and a  $C^\infty$  parametering of the modal TE and TM curves, on the modal surface. We can imagine a 2D parametering by frequency or pulsation  $\omega$ , and ratio  $\frac{a}{b}$ . Indeed, they are the sole continuous parameters, allowing an easy congruence, because, consequence of the limit conditions at interfaces, all electromagnetic functions may generally become discontinuous « one time in their life ».

Given a point  $\mathcal{M}(\mathbf{r})$  inside a constant permittivity medium, and belonging to geometrical space, we describe an associated modal point M in modal space by its coordinates  $M(\omega, \frac{a}{b})$ , intersection of the  $TE(\omega)$  and  $TM(\frac{a}{b})$  curves. As usual, the tangent vectors are defined by  $\frac{\partial}{\partial \omega}$  (resp.)  $\frac{\partial}{\partial \frac{a}{b}}$ .

Knowing that we travel along a mode when we vary the scalar potentials, these vectors may be linked to wave vectors. The  $k_i$  wave vector is fixed and allows to orient the modal space, let it define sometime linked to the local curvature at M. We choose the  $k_z$  one as tangent vector of the TE or TM curve, so  $k_z^{TE} = \frac{\partial}{\partial \omega}$  (so the  $M(\omega, .)$  curve, is merely a dispersion curve), replacing TE by TM for TM mode.

As TE and TM are in principle independent decoupled solutions, there tangent vectors define a basis of the tangent plane at M. So inside that tangent plane which is a vector space, the HE and EH wave-vectors may be defined. A proposal of modal space is given by the figure 1. Here we represent only the frequency sheet.  $\frac{a}{b}$  one may be viewed as travelling along axis, or creating new sheet (non represented). Generalisation to multi-layers drives to higher dimensional manifold, but the concept becomes more intricate<sup>4</sup>.

As we don't examine for now, events before cutoff, we bound the modal space by 2 edges, each for TE and TM. These modes are independent near cutoff, so the edges, parallel to  $k_i$ , then vertical, belong to 2 distinct sheets. The  $\psi$  network must define M with 1-1 correspondence, so the 2 congruences must cross. We have drawn an intermediate point M, where coupling TM/TM starts to be significant. Then  $k_z^e$  and  $k_z^m$ , the projections of  $k_i$

---

<sup>4</sup>except with 3 media, which is out of present publication



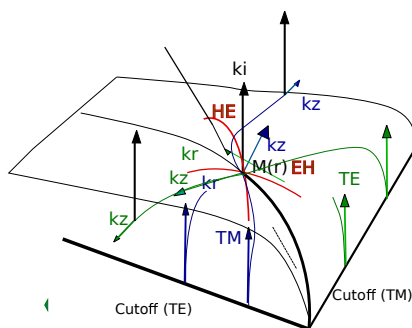


FIGURE 1 : Proposal of modal space

on the 2 congruences, are independent vectors, and define the tangent plane  $T_f(M)$ , where in that basis, we can now define the wave vectors of HE and EH modes (red curves). When frequency raises, as described, the longitudinal wave vectors become parallel, reflecting degeneracy, and their amplitude decreases. The topological structure is here homotopic to a plane.

### 2.3 Basis of VPM

There are several methods for the computation of the fields, by Green functions by the Method of Moments (MoM), Multipole development, by Hertz vector, by Vector Potentials Method (VPM), they may be found in classical references [7]. However, in antenna or wave guide applications, the last method by Vector Potential Method (VPM), partly used by MoM, is well suited for analytical representation<sup>5</sup>

The main principle of VPM is to deduce the fields and potentials of a mode, starting from the axial wave vector, solution of Helmholtz/Maxwell propagation equation. It is detailed in annex.

It is well known that in cylindrical coordinates, the axial vector  $k_z$  decomposes as the complex vector identity,  $k^2 = k_\rho^2 + k_z^2$ , where  $k^2$  only depends on dielectric interfaces. However, as we have many interfaces, the equations are coupled, and non linear, so  $k_z$  of hybrid mode, is for now only computed numerically. The continuity relations bring us to a matrix system  $AC = 0$ , which is inverted to determine the solution(s)  $k_z$ , and the fields coefficients of hybrid mode HE or EH, which are combination of pure TE and TM one.

So knowledge of  $k_z$  allows to describe the transversal field structure of hybrid modes by  $k_\rho$ , which depends on geometry and permittivity of interfaces. That second part may be done analytically, by Maxwell equations, where field components, due to cylindrical symmetry, are expressed by special Bessel functions.

It resumes the minimal algorithm for achieving computation of the potentials/fields and determination of the modes inside a hollow dielectric guide, in the frequency spectrum. There are of course refinements which were added to the algorithm. It will be stressed in the code description, in the second part.

---

<sup>5</sup>Vector Potential Method, as restricted to scalar potentials, does not coincide but share some principles with Hertz Vector theory, see [23]

To be synthetic, the calculus progresses with following steps :

1. input of parameters : permittivity of dielectric layers, n-order of the mode<sup>6</sup>, frequency, geometrical section and length of the guide, ...
2. automatic building of matrix A, given the dimension (number of layers) of the problem
3. solve  $\det A = 0$ , then determination of the longitudinal constant(s) of the modes, and computation of corresponding  $k_{\rho s}$
4. solve  $AC = -a$  to determine the C(s) coefficients
5. analytical computation of the scalar potentials and electromagnetic fields

---

<sup>6</sup>let's recall that the m of  $J/N_m$  coincides with the  $TE/TM_{mn}$  and  $\cos/\sin(m\phi + \dots)$ , where m is the order of the J/N, and n its  $n^{th}$  zero; anyway the situation is less clear for hybrid modes, it deals with their nomenclature. That topic has been evocated in [2.1](#)

### 3 CODE DESCRIPTION

#### 3.1 General

The entire code subdivides into code interface (Gtk+ widgets) for inputting parameters, and calculus in Julia.

It has been designed for local machine, but could be paralleled, Julia offering an -experimental- multi-threading support. Anyway, the total run time for computation of 2 dielectric layers with one frequency is typically  $\mathcal{O}(s)$ , and the procedure is sequential, so for now the translation is not well adapted to parallelism, and it appears not necessary.

Regarding the work amplitude to explore the different physical cases even with 2 media, the present version of the code has been implemented for 2 layers only. Also, acceleration application have been envisaged into a hollow metallized fiber, gained inside with a thin layer, so the configuration is layer1=vacuum, layer2=dielectric, frontier=PEC (Perfect Conductor), which is the 2 layers problem. Additionally, the generalisation for n layers doesn't bring thorny theoretical problems, nor add new physical landscape.

As in Julia, we can manage modules, it will be rather direct to build a new multi layer module for future versions.

The today version subdivides into modules pictured by fig 2

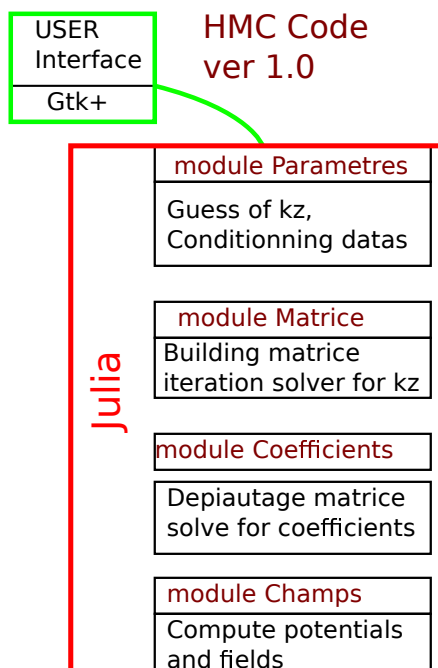


FIGURE 2 : Actual version of code HMC ver 1.0

The following sections describe the different features of the  $\beta$  code, some of these had to be tested in slightly modified fashion comparing to initial fortran code.

### 3.2 Preparation and conditioning of the input parameters

In order to solve numerically  $\det A = 0$  by iteration, it is necessary to feed the code a guessed value of the  $k_z$  longitudinal constant, not too far from the solution. Of course, a trained user, familiar with his physical problem will be able to provide reasonable values, but in the general case, it is difficult to guess it from scratch.

So I tried to help user to dispose of such value, by semi automatic means. To illustrate it, let's choose, as in [4], a 2-layers system, constituted by a central cylindrical dielectric ( $\epsilon = 10$ ) of radius  $a$ , immersed into a hollow cylindrical guide and let's compute  $k_z$  when the ratio  $\frac{a}{b} = \alpha$  grows from 0 to 1. At  $\alpha = 0$ , the configuration is a pure hollow vacuum guide, so  $k_z$  is easily given by  $(k_z)_{1,2} = \sqrt{k_{1,2}^2 - (k_{r=b})^2}$  where  $k_{1,2}^2 = \omega_{1,2}^2 \epsilon_{1,2} \mu_{1,2}$ , and  $(k_{r=b})^2 = k_2^2 - \frac{\eta_1}{b}$ .  $\eta_1 = (1.841)$  is -for instance- the first zero of the derivative of Bessel  $J_1$ .

Conversely, when  $\alpha = 1$  ( $a=b$ ), the guide is filled with dielectric, and the precedent relation leads to  $(k_z)_{1,2} = \sqrt{k_{1,2}^2 - (k_{r=b})^2}$  with  $(k_{r=b})^2 = k_1^2 - \frac{\eta_1}{b}$ .

The corresponding graph of the reference [4] is given by the figure 3

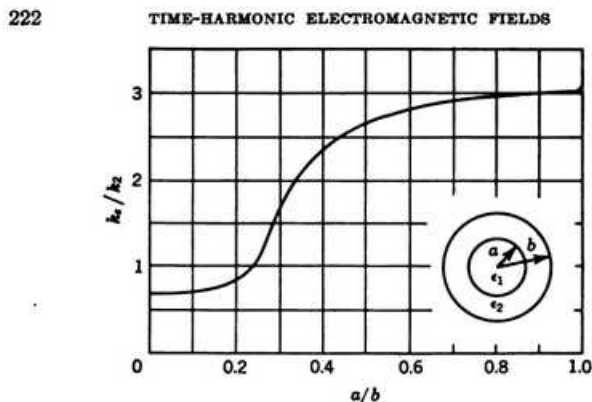


FIG. 5-11. Phase constant for the partially filled circular waveguide,  $\epsilon_1 = 10\epsilon_2$ ,  $b = 0.4\lambda_2$ . (After H. Seidel.)

FIGURE 3 : Graph of  $k_z$  versus  $a/b$

The values of the recording points at  $\alpha = 0$  and  $\alpha = 1$  are correctly restated. Of course, all the curve between these points, subject to hybrid modes, cannot be guessed precisely. All we know is that curve transitions probably smoothly between these values<sup>7</sup>.

There are 2 main tentatives to build an « universal » shape of curve, among them fitting the reference with spline or equivalent numerical method, or defining some analytical empiric relation in some regions of the curve. The spline method has the limitation that it necessitates an experimental or published curve, given the permittivity which can differ from one application to another.

The qualitative approach should be the best one. First constatation is that the curve has generally 1 change of curvature and a part, fastly growing, when the curvature is

<sup>7</sup>in case of inverse problem with  $\epsilon_1 = 1$  and  $\epsilon_2 > 1$ , which is the case with THz projects in hollow fiber, the recording points of the curve may be obviously inverted

quasi null. Secondly, at the neighbouring of limit points, the curve variation is quite low, so we can approximate it by the extension of the pure modes. Saying it differently, for the neighbouring of the limit points, the real mode is close to pure TE11 mode, with modulation of dielectric index. These 2 zones extend relatively far from the limit points.

For the central part, a fast try on an empiric form like

$$f(\alpha) = \frac{\eta_1 b}{b^2 + \exp^{\frac{\alpha^2}{\tau} - 1}} \quad (1)$$

with  $k_z = \sqrt{k_2^2 - (f(\alpha))^2}$  and  $\tau \sim 0.27$  gives approximate fit. Much fundamental effort could be expanded to understand these transitions, for instance by approximations of special functions in adequate domains.

Moreover, when the empiric curve is added to the datas, we need to join it with the precedent low variation segments. It is relatively easy done by the code.

The precedent considerations must not lead us to forget that the built curve is only a help to the user, in order to provide a guess of  $k_z$  not too far from the exact one.

Lastly, 2 additional values aside form that central guessed value of  $k_z$  are determined by a criteria on amplitude variation on the curve. The set of 3 values is necessary for Muller algorithm, see the annex.

### 3.3 Building the matrix and solving for longitudinal propagation constant

Once input datas are defined and first guesses of  $k_z$  by the `modes_parameter` module, they are injected inside the module `mode_matrix`. The module calculates in loop, the final value of  $k_z$  by building at each iteration, the matrix  $A(k_z)$  and computing  $\det(A)$ .

Concerning the coefficients, they are obtained by knowledge of the values of Special Functions like Bessel and Neumann. There is a module `SpecialFunctions` we can import in Julia, but even if it is efficient, based on fortran libraries, it doesn't provide some derivatives.

So you must use mathematical relations to find them. Let's recall [1], and NIST, [13].

We need the values of  $J'_n$  and  $N'_n$ . We use [13] :

$$\mathcal{C}'_\nu(z) = -\mathcal{C}_{\nu+1}(z) + \frac{\nu}{z}\mathcal{C}_\nu(z) \quad (2)$$

where  $\mathcal{C}$  stands for any special  $J_n$  or  $N_n$ , Hankel, ... functions.

Regarding the algorithm of convergence, [26] uses Muller method, which order of convergence may be 1,84. I investigated if other performant numerical methods could be

---

<sup>8</sup>Using that relation, one must take care that  $z = kr$  in our case. Derivation should apply only to  $r$ , so we should have

$$\frac{dJ_n(kr)}{dr} = \frac{dkr}{dr} \frac{d}{dkr} J_n(kr) = k \frac{dJ_n(kr)}{dkr} = k \frac{dJ_n(kr)}{dkr} = k[-J_{n+1}(kr) + \frac{n}{kr} J_n(kr)] = -kJ_{n+1}(kr) + \frac{n}{r} J_n(kr) \quad (3)$$

as or more efficient. Certainly Newton Raphson algorithm has the best order of convergence, 2, but I found no other algorithm than Muller able to deal with complex numbers for transcendental equation  $f(z) = 0$ . Some of them exist but restricted to polynomials[21]. For improvement, an hybrid Muller and bisection method could be to consider [27], because there is a trade-off between order of convergence and stability, we shall see it in results. Also let's mention a complement about searching solutions of  $f(k_z) = 0$ , where  $f$  is transcendental. The main question is not to find an extremum of  $f$ , but to qualify it in scope of physics landscape. Particularly for  $k_z$ , the mode classification is central.

Indeed it is useful to remain that all wave numbers are *a priori* complex one. That feature incorporates the losses by the expression

$$k = \beta + j\alpha \tag{4}$$

So I kept Muller method inside the module, and modified some Muller one for Julia, to deal with complex numbers, and to include the matrix construction.

The Muller method necessitates 3 guesses, like those introduced above. I don't discuss the method, which is largely detailed by numerous references, but I enclose here the figure 4, which depicts clearly the process. To be short, the 3 guesses defines a quadratic curve, which parameters are found by the conditions stated on these 3 points ; at  $x=x_0$ ,  $f(x)=f(x_0)$ , idem for  $x_1, x_2$ . Then 3 equations for a curve  $ax^2 + bx + c$ , allow us to find the free unknowns  $a, b, c$ .

Inside the Muller method, I defined a type Function, and referenced it to the function which build the matrix and computes its determinant. That procedure is very concise, and lightens considerably the writing of the code.

The computation is fast, but must be controlled with the value of increment objective  $\delta$  ( $\delta = x_n - x_{n-1}$ ) and the maximum allowed number of iterations. Like the value of the guesses in precedent module, it constitutes a critical step.

The final value of  $k_z$  is transmitted to the following module.

### 3.4 Calculation of C coefficients

When  $k_z$  is known, we can re build the final matrix A, and proceed to what I call « depiautage »

The « depiautage » uses typically 2 or 3 instructions of Julia. We dispose also of one instruction for the determinant. Anyway, the syntax  $B = \det(A)$  is not so trivial if one goes deeper inside the source. *det* is in fact a collection of very sophisticated procedures, which detect in first the pivots, if the matrix is singular, and make essentially a LU decomposition<sup>9</sup>

Similarly, Algebra science has not evolved fundamentally since the original reference[26], the most reasonable is to proceed to the standard LU decomposition and find the solutions by backward substitution. What is new in Julia, is that you don't need to implement the

---

<sup>9</sup>let's recall that LU is made in the very general case, when the matrix has no symmetry ; in case of any symmetry, *det* branches immediately to the adequate algorithm, ie Cholesky, and so on. . .

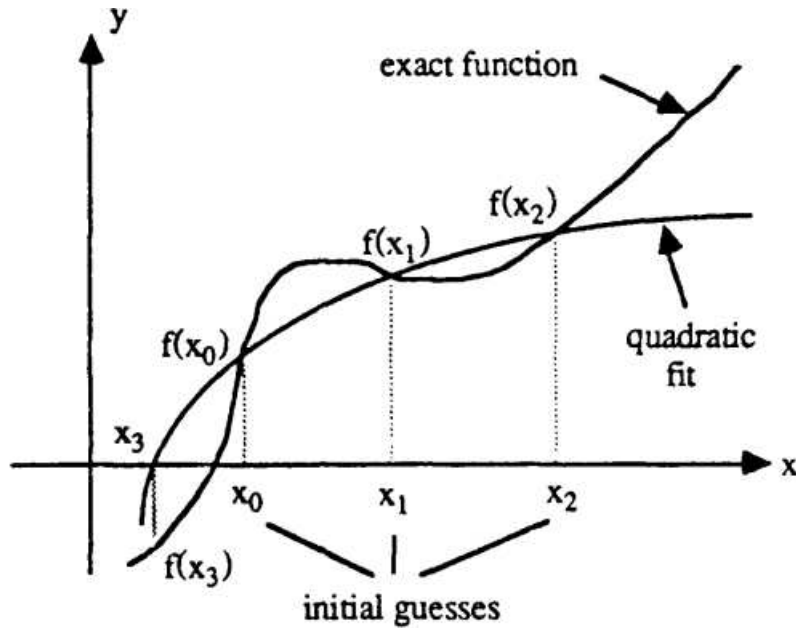


**Figure 3.1. Example of the quadratic fit procedure to locate the zero of a function by Muller's method.**

FIGURE 4 : Principle of Muller method, after [26]

entire algorithm made in coherence with [15] because Julia disposes also of an integrate function, which provides the LU decomposition and -important- the permutation vector of the pivots.

Then if you write  $A'C' = a'$ , by LU you can also classically write  $PA' = LU$ , then  $A' = P^{-1}LU$ , where  $A'$ , respectively  $a'$ , are the « depiautage » of  $A$  and the residue of that operation.  $C'$  is « depiauted » from  $C$  by ignoring  $C_{11}$ .

It follows that  $P^{-1}LUC' = a' \Rightarrow C' = U^{-1}L^{-1}Pa'$ , which gives us  $C'$ . We recover  $C$  from  $C'$ , adding again  $C_{11}$ .

### 3.5 Calculation of scalar potentials and electromagnetic components

That final part should be the less difficult routine. However, first run did reveal a great dump of datas, because user (me) asked for a volume bounded by  $z_{max}$ ,  $r_{max}$ , and  $\phi_{max}$ . Of course, performances of our machines allow such fluxes, but I felt more suited to offer to the user, the possibility to compute a « slice » in  $r$  and/or  $\phi$ . It constitutes a great advantage of the frequency domain, so it is possible to visualise a sector of the fields/potentials ( $z = cste$ ,  $r$  variable,  $\phi$  bounded variable), a section ( $z = cste$ ,  $r, \phi$  variable), a longitudinal profile ( $r, \phi$ , bounded variable,  $z$  variable),...

It is easy to bound  $\phi$  and  $z$ , but for  $r$ , the computation depends on the location of  $r_{\min}$  and  $r_{\max}$  in regard to the multi layer geometry. So before the calculation, the set  $(r_{\min}, r_1, r_{\max}, r_2, \dots)$  must be automatically ordered.

A simple control flow leaded to correct order, and it has been possible to compute  $E$  inside the bounds. For instance, the figure 5 shows a polar plot of the radial component  $E_r(r, \phi, z)$  of a rod of  $\frac{a}{b} = 0.5$  of permittivity  $\epsilon_r = 37.6$  inside a cylindrical guide of  $b = 0.012m$ , at  $frequency = 3GHz$ . The analysis windows are  $r \in [0.2b, 0.7b]$ , and  $\phi \in [0^\circ, 150^\circ]$  and  $z = 0.0$ .

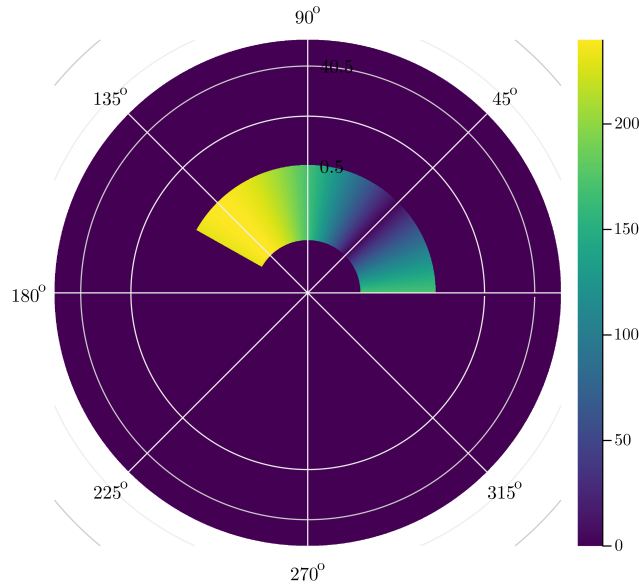


FIGURE 5 : Slice of  $E_\rho$ ,  $b=0.012m$ ,  $a=0.5*b$ , rod of  $\epsilon_1 = 37.6, \epsilon_2 = 1.0, f = 3GHz$



## 4 DISCUSSION

### 4.1 Use of different Special Functions among publications

We have stated that EM fields are solutions of linear combinations of  $J_n$  and  $N_n$  where  $J_n$  and  $N_n$  -last one, Neumann function in [26]- are first and second kind Bessel functions. To precise, these notations refer in recent standard like NIST, to  $J_n$  and  $Y_n$  notations, confirming the validity of the calls in Julia (besselj and bessely routines)<sup>10</sup>.

Also, Hankel functions of first and second kind are sometime cited in literature. In standard NIST notation, they are noted  $H_\nu^1$  and  $H_\nu^2$ , they are called Bessel functions of 3rd kind, and we have

$$H_\nu^{1resp2} = J_\nu + i(resp-)Y_\nu \quad (5)$$

<sup>11</sup>

so there is an equivalence in expressing the fields against Bessel or « Hankel » functions, provided computing different coefficients

However we often find, for example [7], [17], . . . , formulations like

$$E, H \propto AI_n(kr) + BK_n(kr) \quad (6)$$

where  $I_n, K_n$  are described as modified Hankel function of the first, second kind. Again, in actual standard conventions (NIST),  $I_n$  and  $K_n$  are respectively first and second kind **modified Bessel** functions, also identically noted  $I_n$  and  $K_n$ .

[26] describes them in the case of losses, so its formulation is to replace  $J_n$  and  $N_n$  ( $Y_n$ ) by  $I_n$  and  $K_n$ . Let's note that  $I_n, K_n$  do not belong, for [7], . . . , to the case of metallic cylinder dielectric loaded wave guide, but for a whole dielectric cylinder like step index fiber, for example, and it is probable that losses are implicitly taken in account.

Moreover, it is well known [13], that changing the  $z$  in  $iz$  in  $J_n, N_n$ , results in finding linear combinations of  $I_n$  and  $K_n$ . In fact, the choice of different functions -except the trivial possibility to use linear combinations, results essentially from boundary conditions or limit conditions, for example  $K_n$  has a good asymptotic behaviour to 0 at infinity, as radiated field from 2 dielectrics wave guide if no metal shield encloses it.

So, excluding losses, the Whites formulation seems to be coherent. Concerning the accurate study of modes, the case of high losses may be treated in future work.

Finally, the Harrington expressions seems to lead to an identical determinant as those of Whites for 2 dielectric, where the 2 first columns are identical, and Harrington 3rd column should be a linear combination of Whites one.

---

<sup>10</sup>In Abramowitz & Stegun old edition «  $Y_\nu(z)$  is often denoted  $N_\nu(z)$  by physicist and European workers »

<sup>11</sup>of course all the relations of that sections must be viewed in connection with a precise definition domain

## 4.2 Various divergences to [26]

It was noticed some points of divergence :

1. in the 2 dimensional matrix taken as example, page 17, line 5, instead E2 and E4 as defined,  $Jn(k_{\rho 2b}), Nn(k_{\rho 2b})$ ; also in line 6, instead of E'2 and E'4,  $J'n(k_{\rho 2b}), N'n(k_{\rho 2b})$ , last rows  $E2, E4, E'2, E'4$  are calculated with b argument, not a
2. for the derivation seen above, ambiguity between the  $r$  and  $\rho = kr$  arguments
3. idem p17, sign errors in A13,A14,A25,A26,A33,A34,A35,A36

## 5 RESULTS

### 5.1 Characteristic curve $kz = f(a/b)$ for different ratios $a/b$

That step may be very useful, because for the first hybrid modes, like built from TE11, knowing the possible instability of Muller algorithm and its non physical insight, it should be appreciated to have a precise value of  $kz(a/b)$ . However, precise reference of the curve shown in [4], describing  $kz/k_0 = f(a/b)$  for HE11 mode, being an old archive, seems to be difficult to find in the literature. Additionally, it may provide some criteria to access to mode designation, as we shall see.

#### 5.1.1 Numerical method

The **hmc** code finds a first guess of  $kz$ , via a preliminary module, and transmits it to a second module. This last one computes a more precise solution via Muller method. A variant of **hmc** has been automated to output the entire curve  $real(kz)/k_0 = f(a/b)$ . That curve -the phase exponent of  $kz$  viz  $\frac{a}{b}$ - is represented by the figure 7 for the HE11 mode.

Here is represented the following case described by Harrington at the figure 6, where raccording curves is made between the asymptotes of void and filled guide. Here,  $k_i^2 = \epsilon_i \mu_i k_0^2$ ,  $k_0 = \frac{\omega}{c}$  and  $\tau = \sqrt{0.27}$  (see below for definition of  $\tau$ ). Of course it is in addition, necessary to smooth the curve by simple numerical interpolations between its successive points. Given radius  $a$  and  $b$ , a first trio of  $k_z$  guesses is determined on that approximate curve, with a given window (vertical distance between the 3 points).

The used window has been in practice, 10% of the maximum amplitude, around the principal guess. The envelope of the curve approximates correctly the Harrington one. However, numerous accidents occur in the transition zone, when  $\frac{a}{b} \in [0.2 - 0.4]$ . A simple non automated computation for  $a = 0.028$ , then for the first accident of the curve, gave a correct result. It was shown several reasons to these divergences. Firstly, as explained above, some differences are noted with the Thesis in reference [26], specially on Bessel derivatives. Moreover, and it seems to be the main contribution, the convergence test for Muller procedure, dealing with complex numbers, should not be a comparison between the moduli of the successive approximations, but **between their real parts**, knowing that we searched for a real curve in our case. Finally, the determination of successive guesses along the curve is not correct, because it drives to a stair case approximate curve. Last point has been partly enlightened by the simulations of dispersion, see later in the document.

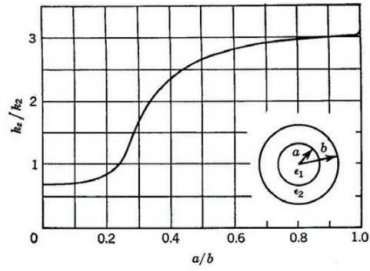


FIG. 5-11. Phase constant for the partially filled circular waveguide,  $\epsilon_1 = 10\epsilon_2$ ,  $b = 0.4\lambda$ . (After H. Seidel.)

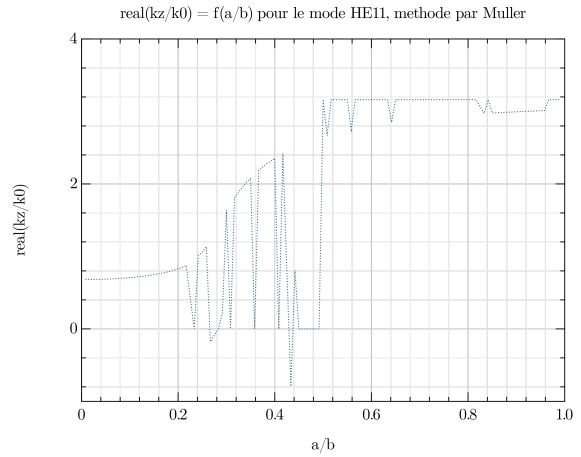


FIGURE 6 : Harrington reference for HE11      FIGURE 7 : First calculation of HE11 mode with a/b variable

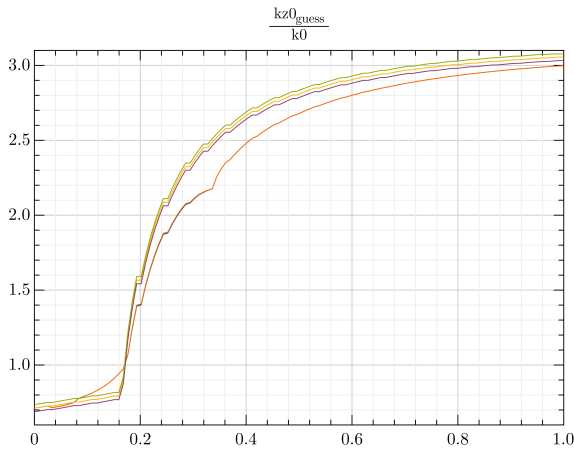


FIGURE 8 : Optimised simulation, with representation of the first guess curves

With the real part comparison criterion, the  $k_z$  values are all real and lie between  $k_1$  and  $k_2$ , with respective values 23 and 62. some analytical fit were tested to give a first starting set of values for numerical guesses. For example :

$$k_z^2 = (k_1^2 - \frac{te11^2}{x^2}) \quad (7)$$

$$k_z^2 = (k_2^2 - \frac{(te11 * b)^2}{(b^2 + e^{\frac{a^2}{r^2}} - 1)^2}) \quad (8)$$

Observation of the « abnormal points » of the first simulation, shows that they are always associated with a significant imaginary part,  $\mathcal{O}(1)$  witch sign may be positive or negative. All other points of the envelope have a negligible imaginary part. As majority of them are situated in the intermediary zone of hybrid modes, when  $\frac{a}{b} \in [0.2 - 0.4]$ , so it exists other solutions, firstly  $EH_{11}$ , radiating modes, and coupling of forward and backward waves inside the 2 media. Hence there is a doubt on the real smooth behaviour of  $HE_{11}$  seen on the literature. A new simulation is driven with the modifications reported above (see figure 8).

We could deduce some analogy with the LP<sub>lm</sub> modes of optical fibers[6]. However, there is a major difference, ie the continuity equation in the last medium. The field is not allowed to extend to infinity, due to metallized external « shooping » of the guide<sup>12</sup>. So there is a possibility to encounter some reflections of the wave, resulting in unwanted coupling, and accidents or abnormalities in the dispersion curve.

---

<sup>12</sup>For particle accelerators, the expansion of electromagnetic fields is to avoid outside of the guide, so the necessity to shield it

### 5.1.2 Help to user : guess of approximate $kz=f(a/b)$ curve

We've seen that a first approximation for lossless media, allow us to inject guesses in the numerical method and retrieve some results of the literature. Is there possible for other more complicated cases?

Firstly, let the solution be  $e^{-jk_z z} = e^{-j\beta z} e^{\alpha z}$  with  $k_z = \beta + j\alpha$  <sup>13</sup>,

1. if  $\beta >, < 0$ , we define a forward, backward wave,
2. if  $\alpha < 0$ , wave is lossy (with proportion to quantify)
3. if  $\alpha > 0$ , wave is of amplifying nature, which we assume non physical<sup>14</sup>

<sup>15</sup>

Let's study the basic fundamental case,  $N = 1$  mode. Given the hybrid mode be a linear combination of  $TE_{11}$  and  $TM_{01}$  for instance, we graph the curves of the 2 basic modes  $k_z$  **function of  $\frac{a}{b}$** , with real and imaginary parts, and for inserting the  $k_i$ . So there are 2x4 cases (real and imaginary),

$$TE_{11}(k_1) = k_1^2 - (te_{11}/a)^2 \text{limit of plain wave guide when a tends to b} \quad (9)$$

$$TE_{11}(k_2) = k_2^2 - (te_{11}/(b-a))^2 \text{limit of void wave guide when a tends to 0} \quad (10)$$

$$TM_{01}(k_1) = k_1^2 - (tm_{01}/a)^2 \text{idem but for magnetic mode} \quad (11)$$

$$TM_{01}(k_2) = k_2^2 - (tm_{01}/(b-a))^2 \quad (12)$$

with multi connecting curves in order not to collapse  $T_{11}(k_i)$  to zero, and an algorithm permitting a soft transition. Moreover, there are 2 cases, depending on  $real(\epsilon_1) > < real(\epsilon_2)$ , in fact, we must chose first and third equations in first case, and second/fourth one, in the second case.

For instance, taking  $TE_{11}(k_1)$ , a transition curve could be

$$TE_{11}(k_1) = k_2^2 - \left( \frac{te_{11} * b}{b^2} + exp\left(\frac{a^2}{\tau}\right) - 1 \right)^2 \quad (13)$$

insuring the dispersion curve to converge to limit value of void wave guide(limit of  $TE_{11}$  void guide, when  $r \rightarrow 0 =$  with  $\epsilon_1 > \epsilon_2$ , example of the rod).

In addition, a fitting transition curve could be, for  $TE_{11}(k_2)$ (limit of  $TE_{11}$  void guide, when  $r \rightarrow 0 =$  with  $\epsilon_1 < \epsilon_2$ , example of the metallized fiber),

$$TE_{11}(k_2) = k_1^2 - \left( \frac{te_{11} * b}{\frac{1}{(b-\tau*a)^2} + exp\left(\frac{1}{(b-\tau*a)^2}\right)} \right)^2 \quad (14)$$

,

<sup>13</sup>arbitrarily by electromagnetic -not quantum- usage

<sup>14</sup>non physical in CW assumption or viz energy balance, but it may easily violate that affirmation in specific conditions, for instance transients, not belonging to the present scope

<sup>15</sup>here,  $\alpha$  is understood to be a gain, contrary to [26]

with  $\tau = 1.01$  and similar algorithm for magnetic case, replacing  $te_{11}$  by  $tm_{11}$ <sup>16</sup>

Taking the following examples in [26] :

Firstly, the Harrington reference, cited above, in order to calibrate our method :

1. a wave guide of  $b = 0.4\lambda$  with  $\epsilon_1 = 1O + 0.0j$ , and  $\epsilon_2 = 1.0 + 0.0j$
2. frequency 1GHz

The testing curves for that example, are reported in the figure 9, where all the expressions are reported.

We see that choosing the curve 1 ( $TE_{11}$ ) and curve 6 ( $TM_{11}$ ), and considering them, seems to reconstitute the searched -approximate- curve<sup>17</sup>.

Another interesting case, for THz and dielectric acceleration with hollow metallic fiber, is when  $\epsilon_1 = 1$  and  $\epsilon_2 = 10$

The curves are represented by the figure 10

Interestingly, the first TM curve is « non physical », which confirm the choice of curves 3,4 and 7,8. We see that again a coherent shape seems to appear for hybrid mode.

Now, let's try lossy materials. Yet with [26], we chose in first, a low loss scenario

1. a wave guide of  $b = 0.5in$  with  $\epsilon_1 = 37.6 - 0.01j$ , with  $\frac{a}{b} = 0.3646$
2. an air 2nd dielectric with  $\epsilon_2 = 1.0 + 0.0j$
3. frequency 4GHz

The curves are now represented by the figures 11

We again observe that the correct determination of low losses modes is curves 1,2 and 5,6. It is interesting to compare them with the same case, but with  $\epsilon_1 = 37.6 + 0.0im$  (no loss). For the null loss case, the real parts are naturally unchanged, and the imaginary one are null (or very low).

Coming back to low losses example, for electric case, as also waited, the imaginary part is notable below the cutoff. When  $\frac{a}{b} > 0.25$ , so with propagation, that part amount to a fraction of unity and is stabilising to a constant. For the magnetic case, it converges also to a constant, but more pronounced. An idea is to assume the searched hybrid mode be a combination of electric and magnetic one, with coefficients resulting of proportions between the phases constants of the two basic modes.

Numerically, let the asymptotes be, as shown in the figure 11  $Im_{electric}(k) \sim 2*10^{-1}$  and  $Im_{magnetic}(k) \sim 5$ , so the ratio between electric and magnetic modes will be  $\frac{e^{0.2}}{e^{-5}} = \frac{1.221}{0.0067} = 181.3$ , which drives us to neglect magnetic component, in the frame of our approximations, so hybrid mode will be very near from electric TE mode<sup>18</sup>.

<sup>16</sup>recall that  $te_{11} = 1.8412$  and  $tm_{11} = 3.8332$

<sup>17</sup>we numerate the curves from left to right and then from top to bottom, so curve 1 is *gre, realTE<sub>11</sub>(k1)* and curve 5 is *ure, TM<sub>11</sub>(k1)*

<sup>18</sup> $\alpha > 0$  for TE mode, normally non physical -amplifying- solution, but is low, so we make the hypothesis that there has been an energy exchange from magnetic to electric mode, and it does not contradict the fact that TM mode is negligible

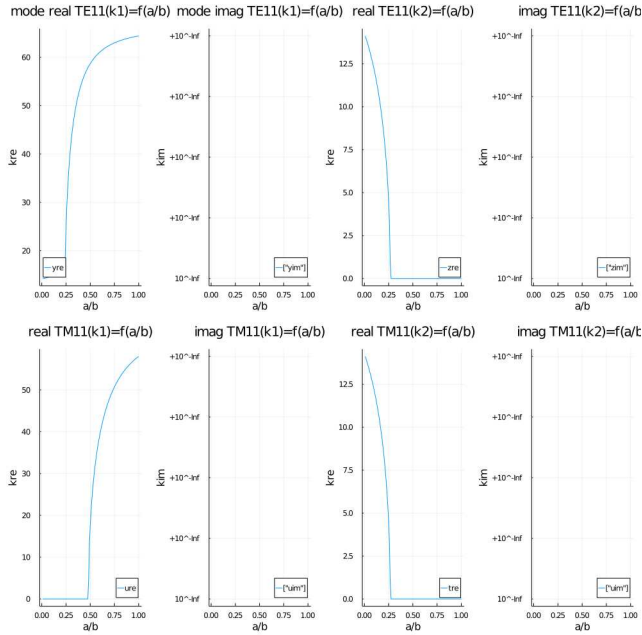


FIGURE 9 : Real and imaginary parts of TE11 and TM11 modes[26]

We now, take a case of high losses material<sup>19</sup>.

1. a wave guide of  $b = 0.6916in$  with  $\epsilon_1 = 23.9 - 15.296j$ , with  $a = 0.5008in$
2. a Teflon dielectric of width  $b - a = 0.1908in$  with  $\epsilon_2 = 2.1 + 0.0j$
3. frequency 3GHz

The curves are reported by the figure 12, see curves 1,2 and 5,6

Above cutoff, TE mode occurs with quasi null attenuation. Magnetic mode experiences a high attenuation with a coefficient  $\beta > 10^3$  so here also, TE mode is predominant.

In summary, for 2 media :

1. depending on whether  $\epsilon_1 > \epsilon_2$  or  $\epsilon_1 < \epsilon_2$  we have to deal with curves 1,2 and 5,6 or 3,4, and 7,8,
2. having determined the correct quattuor of curves, we inspect the values of imaginary parts ; in many cases, we can consider that the predominant mode will emerge in a ratio characteristic of corresponding losses of basic TE and TM components,
3. in specific configurations, the weights of TE and TM components may be equivalent ; hypothetical method -to verify- should be to combine them with coefficients approaching their respective exponential loss

<sup>19</sup>just taken here for demonstration of classification, because rigorously we should replace also the Bessel functions by the modified one, in order to compare



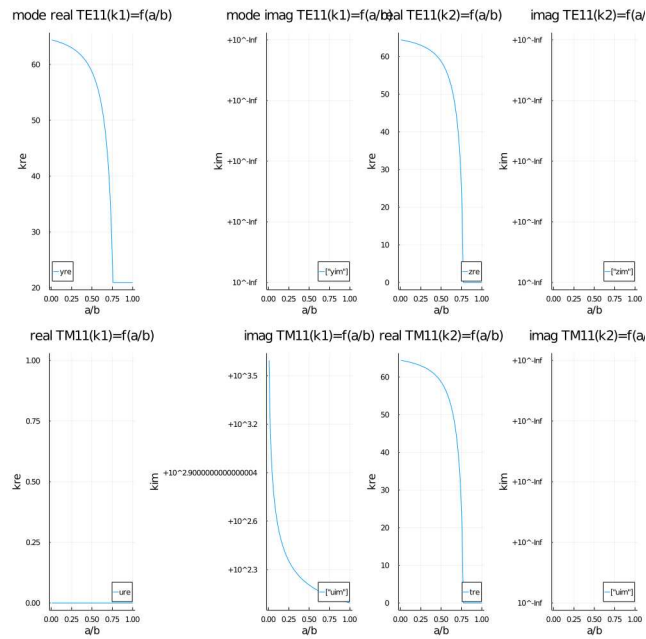


FIGURE 10 : Real and imaginary parts of TE11 and TM11 modes, inversion of indexes

That qualitative procedure seems not to have been reported still now, and may be further automated inside the code. Also, the functions coded for losses materials have been made coherent with those originally intended for no losses.

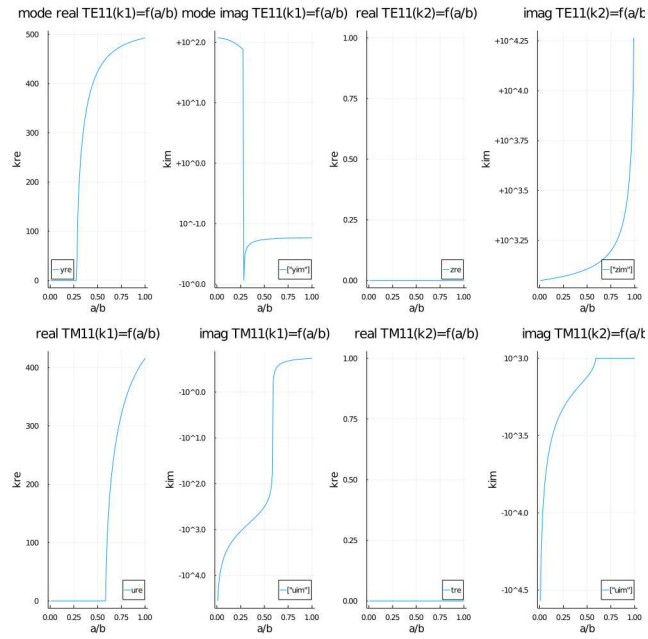


FIGURE 11 : Low losses with  $b = 0.5in, \epsilon_1 = 37.6 - 0.01j, \frac{a}{b} = 0.3646, 4\text{GHz}$  [26]

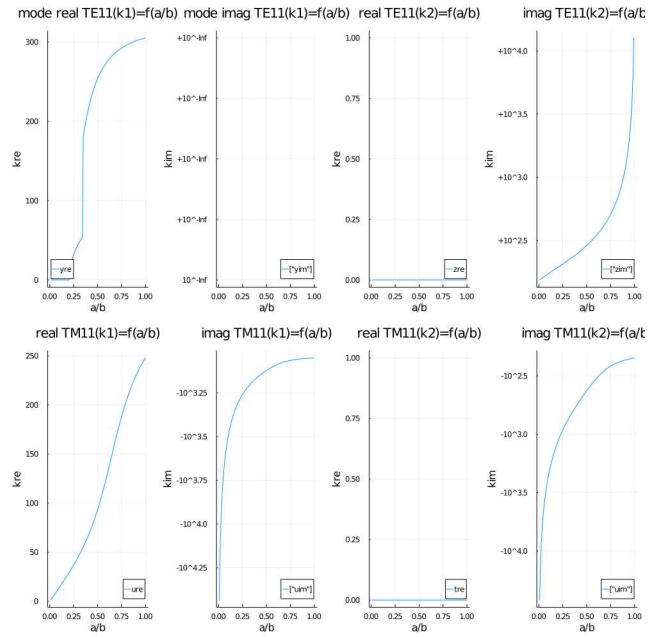


FIGURE 12 : High losses with  $b = 0.6916in, \epsilon_1 = 23.9 - 15.296j, a = 0.5008in, 4\text{GHz}$  [26]

### 5.1.3 Analytical method

Starting from the determinant in [4], we can try to compute it analytically for  $n = 1$ , ie for the  $HE_{11}$  mode.

We found explicitly

$$kz = \pm \frac{\omega a |k_1 k_2|}{k_0^2 \sqrt{F_1 * F_2 * F_3 * F_4}} \sqrt{\epsilon_2 k_{\rho 1} F_1 * F_3 - \epsilon_1 k_{\rho 2} F_1 * F_3} * \sqrt{\mu_2 k_{\rho 1} F_2 * F_4 - \mu_1 k_{\rho 2} F_2 * F_4} \quad (15)$$

20

with the Harrington notations, ie

$$F_1 = J_1(k_{\rho 1} a) \quad (16)$$

$$F_2 = F_1 \quad (17)$$

$$F_3 = J_1(k_{\rho 1} a) N_1(k_{\rho 2} b) - N_1(k_{\rho 2} a) J_1(k_{\rho 2} b) \quad (18)$$

$$F_4 = J_1(k_{\rho 2} a) N_1'(k_{\rho 2} b) - N_1(k_{\rho 2} a) J_1'(k_{\rho 2} b) \quad (19)$$

with « ' » denote derivation in the argument  $z = kr$ . So we need inside the code, the derivatives of  $J_1$  and  $N_1$ , which we find applying successively the recurrence relation for Bessel functions cited before. However, the characteristic equation is of course implicit in addition to transcendental, because  $kz$  appears in arguments such  $k_{\rho i} r$ . Indeed let's recall that  $k_{\rho i} = \sqrt{(k_i^2 - kz^2)}$  with  $k_i^2 = \epsilon_i \mu_i \omega^2$ .

Knowing the approximate range of  $kz$ , we can solve numerically the dispersion relation, and find the curve point by point. The procedure is based on interpolation : at each  $a/b$  ratio, we try  $kz$  from 0 -where obviously  $|kz| < |f(kz)|$ - with positive step, to a threshold until  $kz = f(kz)$  (or  $|kz - f(z)| = o(|kz|)$ ) where  $f$  is our dispersion formula above.

The first results lead to high values of  $kz$ , compared to the reference and results above, and it has to be continued. Also, the numerical trick used, makes travel across the value  $k_2$  where argument is null, so there are divergences of the analytical approximation. That value must be bypassed by the algorithm.

Finally no general analytical method seem to have been reported for high order modes, so it presents a reduced interest.

---

<sup>20</sup>where the  $\pm$  suggests a double direction of propagation

## 5.2 Dispersion curves

Until now, we used largely the [26] results for a/b curves. In that reference, question arose about  $kz = f(\omega)$  curves, ie dispersion curves, and it was eluded by a trick consisting instead of a/b, to define the quantity  $\frac{\omega}{\alpha c}$  where  $\alpha$  is a convenient parameter, and c the light speed in vacuum. However, it is claimed to work if  $\epsilon\mu_i$  do not change -which is the case for the moment- but more delicate, the direct link between both quantities appears not to be so simple.

For example, let's consider even the first EM mode,  $N = 1$ , and a radius a **not** equal to extreme cases of  $a \sim 0$  (void dielectric, or  $a \sim b$  (full dielectric rod). It is clear that the a/b point coincides neither with pure TE nor with pure TM, but is a combination of both of them, with no trivial coefficients. In other point of view, the kz of pure TE mode, parameterised by frequency for any a, lies in dispersion curves forming a congruence in a manifold, and so lies those of TM mode, so the hybrid solution follows a -frequency or a/b- path in that complex space. The essence of the complexity is the parametering of that topological manifold. Geometrically a/b and  $\omega$  parameters define mappings which are not belonging to the same congruences.

Many other publications, for planar geometries [20], or cylindrical one [4], [20], witness numerical methods only. In fact, as the zeros of  $J'_\nu$  and  $J_\nu$  are alternate, it is suggested as in a/b approach, to build a guess curve, intermediate between 2 modes, and solve exactly by Muller method. For example, for the N=1 mode, we could consider a combination of  $TE_{11}$  and  $TM_{11}$  modes.

Recalling that

$$k_z^2 = (\epsilon\mu)_i \left(\frac{\omega}{c}\right)^2 - k_\rho^2 \quad (20)$$

<sup>21</sup>,

and  $k_{rho} = \frac{\tau_{vij}}{(aOrb-aOrb)^2}$  these curves behave like  $\pm\sqrt{(px^2 - q)}$ , ie a quasi linear shape as x high, and a real part above  $x = \sqrt{qp}$ , which is the cutoff frequency condition. Let's guess a law like  $k_z^{HE} = uk_z^{TE} + vk_z^{TM}$ ,  $k_z^{EH} = k_z^{TM}$  and try  $u = v = \frac{1}{2}$ . accounting the fact that TM  $\beta$  curve for first mode, is under TE one, it ensures that HE lies inside both pure modes, and EH under TM one.

Simulations have been made for the scenario of [26], ie  $\beta - \omega$  curves for a rod-insert guide, having  $\frac{a}{b} = 0.788$ ,  $b = 0.5in = 0.012m$ ,  $\epsilon_1 = 37.6 + 0.0j$ ,  $\epsilon_2 = 1 + 0.0j$ , and  $\mu_i = 1 + 0.0j$ . Dispersion results are conform to his reference curve fig 3.10. However, it is often necessary to start near of the exact  $k_z$  solution, to apply Muller method, and in this case, even starting from the TE11 curve, which is very close to HE11 one, sometime the solution forked abruptly to other values, EH11, and even complex kz. These results are interesting because we should like to gather every kz(s), but we loose control on the sole HE11 dispersion curve.

So we tried a first coarse scan firstly, for instance, from  $\frac{k_z}{40}$  to  $3 * k_z$ , and computed the determinant of the matrix, which determinant is expected to be null or minimum. The corresponding curve is shown at fig 13, for  $f = 3GHz$ , and in the same conditions of [26].

---

<sup>21</sup>where  $(\epsilon\mu)_i$  is a short for  $\epsilon_i\mu_i$

It is noticeable that large values of  $kz$ , above say 500, are to remove. Intuitively but with no demonstration of that,  $k_z$  being the image of the axial propagation speed, should be probably less for the hybrid mode, than for the pure TE one, as described above, the 2 speeds should be near, at higher frequencies.

The region below  $k_z = 500$  is interesting. A first minimum is found, corresponding to HE<sub>11</sub>, at approximately 300. A 2<sup>th</sup> minimum appears near from 200, probably due to EH<sub>11</sub>. At last, there should be a -non waited minimum- near 50, at low  $k_z$ . It signs the existence of a new mode, which origin has to be explored, if there is no numerical artefact. Note that with Muller method, we has confirmed the values of 301 and 228, for respectively  $HE_{11}$  and  $EH_{11}$  modes<sup>22</sup>. Our scan differs notably from, and is more general than the method of [26]. That last one aims to add some losses (via the permittivity) to break the mode degeneracy in the  $k_z$  computation. Let's note also, that excepting the minima, all the region below 500 is characterised by very low determinant values. We suspect that it could be the zone of continuous modes, knowing that the modal pure basis is incomplete, and the complete infinite basis, with a proper frequency domain and the usual norm, immerse us into at least an Hilbert space.

In order to automate the process, the following of the method should be directly inspired :

1. to proceed to a  $k_z$  scan in the entire frequency interval,
2. to gather **all** the eigen values of  $k_z$ , at each frequency of the domain,
3. to represent all of them on a  $k_\omega$  graph

Then we are able to compute by Muller the precise values, restricting us to one-to-one intervals with more precise guesses, and a general view on the dispersion behaviour.

That will be one of the topics TODO for next.

## 5.3 Computation of electromagnetic fields and potentials

### 5.3.1 Lossless example, dielectric rod guide at 1GHz

The lossless example of [26] is taken for comparison.

The loss modulus of precedent part for evaluating the longitudinal propagation exponent  $kz$  has been also ported for lossless case, and the results of dispersion curve are very close to Whites and Harrington data.

They are reported in the table hereunder :

| a/b | $kz/k_0$ | $kz$  | $k_{ro1}$ | $k_{ro2}$ |
|-----|----------|-------|-----------|-----------|
| 0.1 | 0.70799  | 14.82 | 64.55     | 14.79     |
| 0.2 | 0.828    | 17.35 | 63.91     | 11.73     |
| 0.3 | 1.638    | 34.32 | 56.64     | -j27.192  |
| 0.4 | 2.354    | 49.31 | 44.21     | +j44.64   |

---

<sup>22</sup>we find different values, 301 viz 312 depending on whether we test the real value or the absolute one into Muller procedure; it has to be cleared

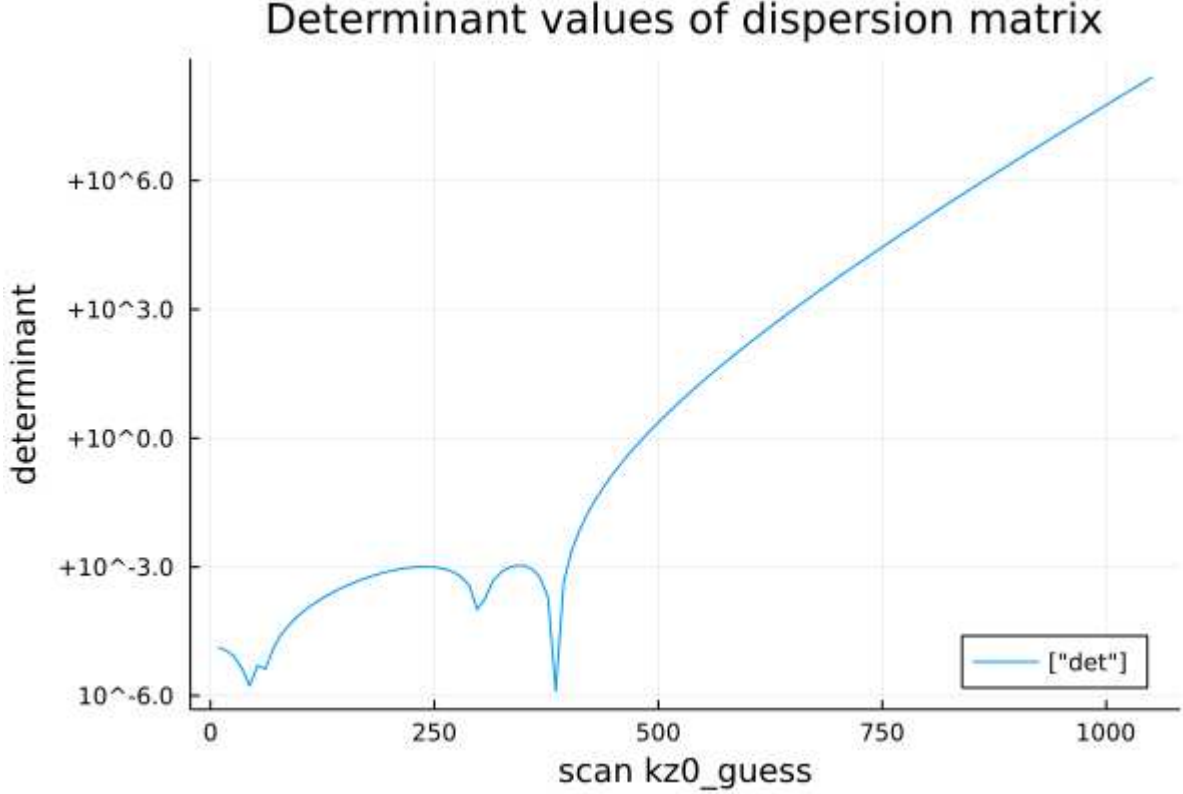


FIGURE 13 : Scan of kz values at a fixed frequency

Knowing that  $k_0 = 20.943$ ,  $k_{ro1} = \pm\sqrt{(k_1^2 - k_z^2)}$ ,  $k_{ro2} = \pm\sqrt{(k_2^2 - k_z^2)}$ , and  $k_i^2 = \epsilon_i \mu_i k_0^2$ , all values of  $k_z$  agree well with [26] but in the last case, the code chose the plus sign for  $k_{ro2}$ , so selecting values must be with care. Indeed, Helmholtz equation gives right to both solutions.

The computed electric fields, see fig 14, 15, 16 and 17, even with the changed sign for  $a = 0.4b$ , gave a correct accordance with the reference publication, but one must keep aware of it for more complicated case, essentially because of the qualitative physical image, of a « radially propagating » component.

We give also the computed magnetic fields, see fig 18, 19, 20 and 21, which shows that these fields concentrate close to the first dielectric with low values of  $a$ , and are moving near the frontier  $b$ , when  $a$  is rising.

All the curves are relative to HE11 mode, as  $n = 1, m = 1$  and HE depends on the sign of the ratio  $\frac{C_{11}}{C_{13}}$ , here positive (Snitzer convention, as cited by [26]).

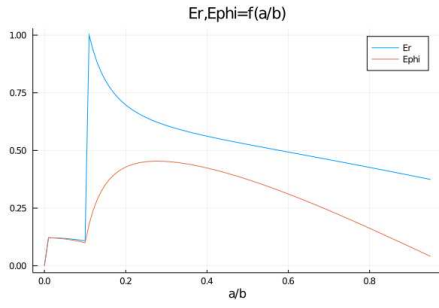


FIGURE 14 : Frequency 1GHz,  $b = 0.4\lambda$ ,  $\epsilon_1 = 10$ ,  $\epsilon_2 = 1$ ,  $\mu_1 = \mu_2 = 1$ ,  $a = 0.1b$

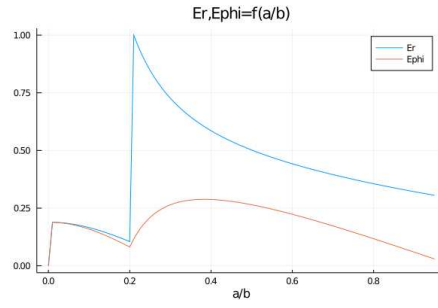


FIGURE 15 :  $a = 0.2b$

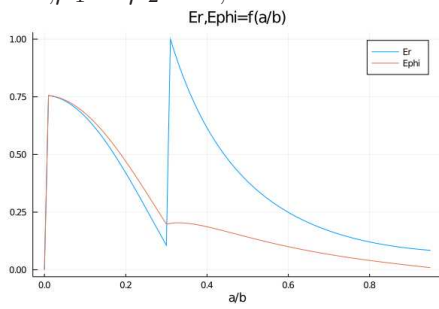


FIGURE 16 :  $a = 0.3b$

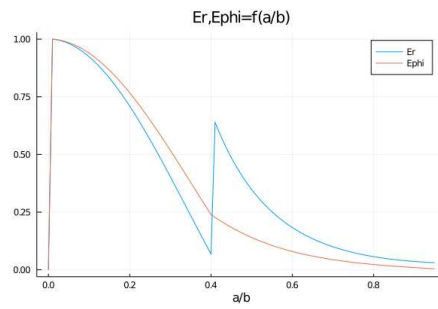


FIGURE 17 :  $a = 0.4b$

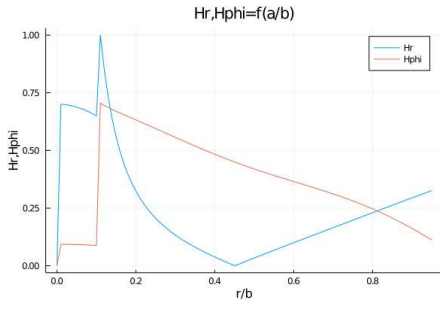


FIGURE 18 : Frequency 1GHz,  $b = 0.4\lambda$ ,  $\epsilon_1 = 10$ ,  $\epsilon_2 = 1$ ,  $\mu_1 = \mu_2 = 1$ ,  $a = 0.1b$

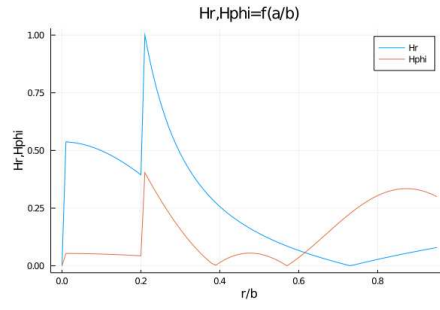


FIGURE 19 :  $a = 0.2b$

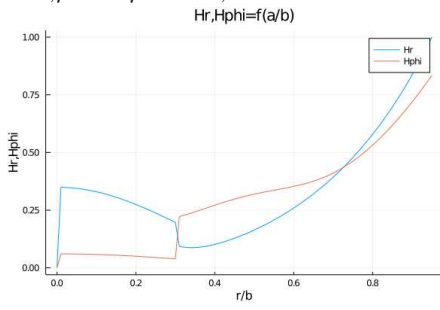


FIGURE 20 :  $a = 0.3b$

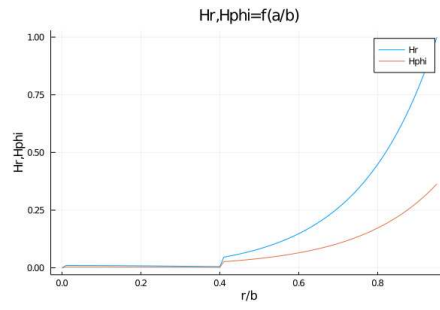


FIGURE 21 :  $a = 0.4b$



The z-fields are given by the figures 22 for  $E_z$  and 23 for  $H_z$ , for  $a = 0.4b$ . The accelerating field is maximum at  $r = 0.4b$ , more generally at the frontier of the 2 dielectrics, but not efficient for  $r \neq a$ . Above dielectric 1,  $E_z$  is fastly decreasing. The magnetic field is efficient at the frontier between the 2 dielectrics, but not active inside  $r < b$ . That consideration may be transposed for other values of  $a$ .

Let's recall that the present configuration pertains to the rod of radius  $a$  and  $\epsilon = 10 + j0$  inserted inside vacuum  $\epsilon = 1 + j0$ . That consideration may be transposed for other values of  $a$ .

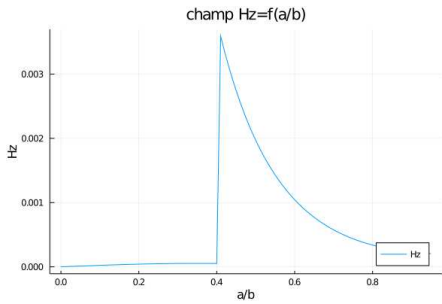
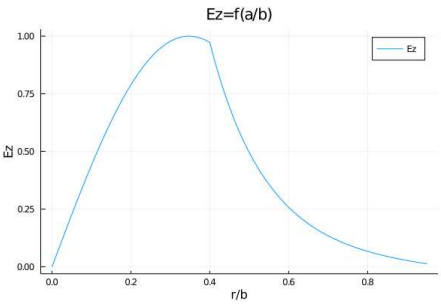


FIGURE 22 : Frequency 1GHz,  $b = 0.4\lambda$ ,  $\epsilon_1 = 10, \epsilon_2 = 1, \mu_1 = \mu_2 = 1, a = 0.4b$       FIGURE 23 : Frequency 1GHz,  $b = 0.4\lambda, \epsilon_1 = 10, \epsilon_2 = 1, \mu_1 = \mu_2 = 1, a = 0.4b$

### 5.3.2 Bounded guide, example in THz region

Our application is pertaining to dielectric acceleration, THz or photonic one, inside a Dielectric coated Metallic Hollow Fiber DMHF,[24] and we can select for example

1. frequency 300GHz,
2.  $b = 0.4\lambda$
3. metallized coating of width  $\frac{\lambda}{10}$

A first exploration gives us the HE curve 24, which is represented hereafter.

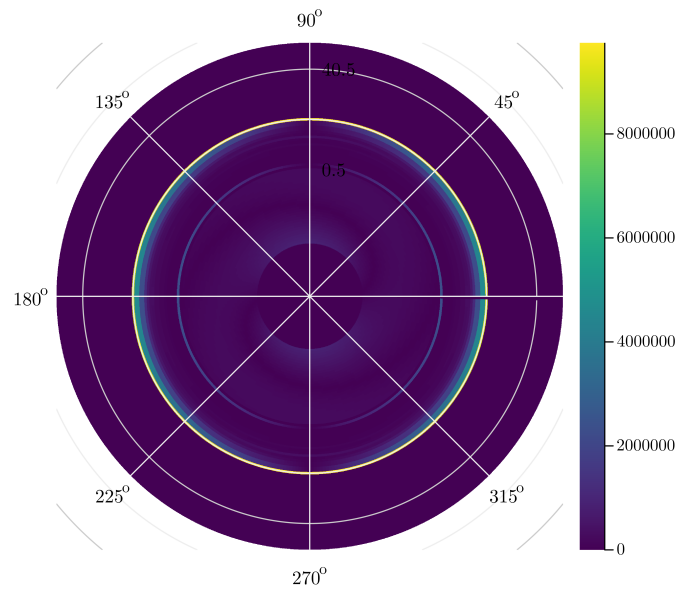


FIGURE 24 :  $E_{rho,HE}$  mode, fiber  $b = 0.4\lambda$ ,  $f = 300GHz$ , rod 0.6mm,  $\epsilon_1 = 37.6, \epsilon_2 = 1.0$

Some recent interesting researches deal with « colossal epsilon », so we can retain a classical material, such as silicium ( $\epsilon \sim 10 + j0, \mu = 1 + j0$ ) and LSNO [10], see their figure 4, which -however perhaps non ecological- is described essentially non magnetic in THz range and presents approximately  $\epsilon = 100 + jx$  and  $\mu = 1 + j0$  under 1THz. Losses are not clearly explained, but it is hoped to be reduced. Phonon resonances being higher in frequency range, we could also expect no non linearity, it is to be confirmed by tests in THz dielectric acceleration environment. Another limit of VPM theory is Maxwell Wagner relaxation induced by charges interfaces, in fact Maxwell equations must be corrected to include second terms with charges and possibly currents. However, if it is neglected/not useful, the actual code could be adapted to multi dielectric media.

## 6 PERSPECTIVES

These studies may bring some insights in the particle acceleration topic, linked with dielectric techniques; they may generate new questions.

### 6.1 Elliptical guides

Preoccupations for elliptical guides occur due to 2 factors :

1. it is difficult to fabricate perfect circular guides in large lengths,
2. elliptic sections are in contrary, intentionally made for enhancing field polarisation
3. polarised fields may constitute an attractive feature in accelerators

Integration of elliptical geometries is not direct inside HMC; it asks to add modules for taking account Mathieu-Hill equations. However the formalism is driven once more by Maxwell and eigen solutions by numerical techniques.

### 6.2 Losses

Given the « short » lengths of fibers in known planned experiments, losses could be studied in the frame of quasi no loss approximation. However, in accurate designs, more studies are necessary, and HMC may be optimised without much work to accommodate for them.

### 6.3 Magnetic materials

This seems an important topics, because of presence of magnetic devices, either for focusing<sup>23</sup>, and the necessary magnetic impedimenta (vacuum, power,laser fields, . . . ) surrounding the accelerating guide. The formalism of magnetic guides is to compare with [19], who made an interesting analysis of magnetic driven modes inside rectangular and circular ferrites. For circular one, the classifications based on Polder tensor leads us to some precautions to classify the modes. Here also, work may be conduct with HMC « greffons ».

### 6.4 Multi-layer extension

The THz accelerator applications are less oriented to multi-layer than photonic one. It is why HMC has primarily be designed to bi-layer anlysis, as [24]. However, it is planned to cover the ability of multilayer simulations.

### 6.5 Frequency dependant permittivity

It is certainly a hot aspect to improve in the code, and it is in course.

---

<sup>23</sup>but tomorrow replaced by photonic techniques

## 7 CONCLUSION

The present version of HMC code aims to contribute to diagnosis of mode propagation inside cylindrical guides filled with dielectric. Strong emphasis was made on the search for axial propagation coefficients, which conditions the determination of the hybrid modes. It is then the main contribution of our publication. It seems possible to proceed to a systematic scan of solutions with an enough large window, and then to refine to exact solutions with Muller method.

The code may further improve in many sides :

1. setting up entirely the USER interface, (only feasibility obtained)
2. improving the semi automatic help for  $k_z$  guess,
3. generalising computation to multi layer  $n_{layer} > 2$
4. providing files and plots of field components, power, potentials,...

Most of these « ToDo » are only time dependant, not really conceptually difficult, except the second tasks (semi automatic help).

The tools applied to that type of problem are certainly translatable to other geometries, for instance rectangular guides, even if the codes may be entirely different, the architecture may remain with a USER interface and Julia code in modules.

Among improvements, -even if I investigated optimisations- the quality of programming has to be greatly evolved, taking advantage of the best features of Julia : polymorphism, memory optimisation, speed, object orientation,...

Another application of the code is standing waves in cavities, where HMC could help designers as soon as they keep symmetry. The feature of HMC is of course 3D, but restricted to academical problems. It is stressed here that academic approach may contribute to the RF and photonics expertise for accelerators.

# Annexe

Maxwell equations are developed in frequency domain, in homogeneous media :

$$\nabla \wedge E = -j\omega\mu H \qquad \nabla \cdot H = 0 \qquad (21)$$

$$\nabla \wedge H = (\sigma + j\omega\epsilon)E + J \qquad \nabla \cdot D = 0 \qquad (22)$$

Where J gathers all current sources (deliberately, J is not detailed, because it may designate different sources depending on the application).

The vector potential concept, restricted to  $\psi$ , A is well known. However, let recall it before generalising.

from  $\nabla \cdot H = 0$  we deduce that  $H = \nabla \wedge A$ , where A is a magnetic vector potential. But  $\nabla \wedge E = -j\omega\mu H$  implies that the quantity  $(E + j\omega\mu A)$  is a gradient, namely  $E = -j\omega\mu A - \nabla\psi$ .  $\psi$  is as usual the electric scalar potential. We have to better define A.

Reporting into the  $\nabla \wedge H \dots$ , and neglecting  $\sigma$  in an homogeneous dielectric like material, we have

$$\nabla \wedge \nabla \wedge A = J + j\omega\epsilon(-j\omega\mu A - \nabla\phi) = J + k^2 A - j\omega\epsilon\phi \qquad (23)$$

where  $k = \omega\sqrt{\epsilon\mu}$ <sup>24</sup>.

Using the identity  $\nabla \wedge \nabla \wedge A = \nabla(\nabla \cdot A) - \Delta A$ , we have :

$$\nabla(\nabla \cdot A) - \Delta A - k^2 A = J - \nabla\phi \qquad (24)$$

, so we are free to choose A as  $\nabla \cdot A = -j\omega\epsilon\phi$ .

Now we can write :

$$E = -j\omega\mu A + \frac{1}{j\omega\epsilon} \nabla(\nabla \cdot A) \qquad (25)$$

$$H = \nabla \wedge A \qquad (26)$$

Which expression looks familiar. Actually, Since Maxwell it is guessed that the electromagnetism has a strong duality feature<sup>25</sup>. So we have yet restricted our discussion to electric current sources, but now we can superimpose magnetic current sources. We know that in that case, Maxwell equations grow by the term M, where :

$$\nabla \wedge E = -j\omega H - M \qquad (27)$$

We then define the new Electric **vector** potential F by  $E = -\nabla \wedge F$ , where we see [4] a symmetrical correspondence between electric and magnetic relations. All the fields E and H may be computed now from the vector potentials A and F. Here, the reference

---

<sup>24</sup>and where we chose more convenient the notation « k », instead of «  $\beta$  », which last one is taken as loss coefficient by  $k = \alpha + j\beta$ ; so  $\frac{k}{k_0}$  shall denote the effective index,  $n_{eff}$

<sup>25</sup>excepting the magnetic mono pole

table has been reported :

|                            |                 |
|----------------------------|-----------------|
| E                          | H               |
| H                          | -E              |
| J                          | M               |
| A                          | F               |
| $\sigma + j\omega\epsilon$ | $j\omega\mu$    |
| k                          | k               |
| $\nu$                      | $\frac{1}{\nu}$ |

where  $\nu = \sqrt{\frac{\mu}{\epsilon}}$  is the wave impedance.

Then the total electric and magnetic fields are the superposition of electric and magnetic solutions, and from the relations deduced identically from, and by analogy with, the preceding steps, we finally find :

$$E = -\nabla \wedge F - j\omega A + \frac{1}{j\omega\epsilon} \nabla(\nabla \cdot A) \quad (28)$$

$$H = \nabla \wedge A - j\omega F + \frac{1}{j\omega\mu} (\nabla(\nabla \cdot F)) \quad (29)$$

## .1 Solutions E,H in cylindrical coordinates

We can easily show that F and A are solution of wave equation, ie  $\Delta A, F + k^2 A, F = 0$ . So finding solutions A,F allows us to compute E,H.

In the particular case of pure TE/TM mode, and for i th concentric dielectric of the guide, setting  $(r, \phi, z)$  for cylindrical coordinates, we can choose the couples

$$F_i = 0 \quad A_i = \mathbf{z}\psi_i^m \text{ for magnetic potentials} \quad (30)$$

$$F_i = \mathbf{z}\psi_i^m \quad A_i = 0 \text{ for electric potentials} \quad (31)$$

26

With these choices, we find easily for the cylindrical field components(wher for the moment we have not added the dielectric layer index) :

| Magnetic solution, E   | Magnetic solution, H                     | Electric solution, E                      | Electric solution, H  |
|--|--|---|---|
| $E_r = \frac{1}{j\omega\epsilon} \partial_{rz}^2 \psi^m$           | $H_r = \frac{1}{r} \partial_\phi \psi^m$ | $E_r = -\frac{1}{r} \partial_\phi \psi^e$ | $H_r = \frac{1}{j\omega\mu} \partial_{rz}^2 \psi^e$           |
| $E_{phi} = \frac{1}{j\omega\epsilon r} \partial_\phi^2 \psi^m$     | $H_{phi} = -\partial_r \psi^m$           | $E_{phi} = \partial_r \psi^e$             | $H = \frac{1}{j\omega\mu r} \partial_{rz}^2 \psi^e$           |
| $E_z = \frac{1}{j\omega\epsilon} (k^2 \psi + \partial_z^2 \psi^m)$ | $H_z = 0$                                | $E_z = 0$                                 | $H_z = \frac{1}{j\omega\mu} (k^2 \psi + \partial_z^2 \psi^e)$ |

<sup>26</sup> $\mathbf{z}$  is typed in bold for a vector notation ; then  $\psi = \psi(r, \phi, z)$ , is a scalar function. A and F are vectors. So  $A = (0, 0, \psi(r, \phi, z))$  for instance

where the notation is  $\partial_{xy}^2 \equiv \frac{\partial^2}{\partial xy}$ . Magnetic solution is known as the TM mode, and electric one as TE mode. Then  $E, H_{hybrid} = \lambda E, H^{TM} + \eta E, H^{TE}$  where  $\lambda, \eta$  are coefficients to be determined. Here, all  $\epsilon, \mu, \psi, E$  and  $H$  must be understood with the index of the  $i$  th dielectric.

## .2 The guide is finite/infinite

Here our approach is splitting into 2 directions :

1. the length  $l$  of the guide is finite
2. the length  $l$  of the guide is infinite

In the first case, the guide constitutes a cavity (intentional or not). The longitudinal constant of propagation  $k_z$  are then discrete and quantified by  $k_z l = m\pi$ . The mode are also hybrid but a new index is added, ie  $p$ . This case is of course very interesting for acceleration purposes (for instance standing wave acceleration), but was let temporally apart for studying the second case.

If  $l = +\infty$ , ie the second case, the determination of  $k_z$  is discussed in the following parts. The acceleration applications are also important (travelling wave), knowing that today their techniques distributes almost equally between standing and travelling modes. In certain cases, a proportion of standing wave is also added in travelling techniques.

## .3 Derivation of the superposition coefficients

We have seen that the hybrid modes are a linear combination of TE and TM modes. Then the coefficients must be determined, but better than that, we can determine the scalar potentials  $\psi^e$  and  $\psi^m$  in hybrid configuration, as superposition of the « pure »  $\psi^e$  and  $\psi^m$  of the TE and TM modes, and apply directly the precedent relation to find  $E, H$ , so the coefficients searching approach is now applied on the  $\psi$  functions. In that configuration, we shall rather have :

$$\psi^{e,m} = \lambda_{e,m} \psi^{TE} + \eta_{e,m} \psi^{TM} \quad (32)$$

$$E^{tot} = E^e + E^m \quad (33)$$

where the scalar potentials are superposition, but fields are simply the sum of corresponding electric and magnetic modes

We can easily show [7] that any such scalar potential  $\psi$  is also solution of the wave equation, say  $\Delta\psi + k^2\psi = 0$ .

In cylindrical coordinates, the equation is separable, and the guessed scalar solution  $\psi$  is known to be

$$\psi_n^i(r, \phi, z) \equiv A(r) * B(\phi) * C(z) = J_n, N_n(k_r^i r) * \cos(n\phi) * e^{-k_z^i z} \quad (34)$$

Here  $J_n, N_n$  are respectively Bessel and Neumann functions of  $n$  order<sup>27</sup>, and the wave equation induces the relation :

$$(k^i)^2 = (k_r^i)^2 + (k_z^i)^2 \quad (35)$$

$k^2 = \omega\sqrt{\epsilon\mu}$  is the wave number of the total propagation, decomposing into a radial wave number  $k_r$  and a longitudinal wave number  $k_z$ , the index  $i$  being relative to the  $i$ th dielectric.

Taking the notations of [26], and establishing the continuity relations of the E,H components tangent to the dielectric surfaces, let

$$\dots \psi_i^m = [C_{i1}J_n(k_r^i r) + C_{i2}N_n(k_r^i r)]\cos(n\phi)e^{-k_z z} \quad (36)$$

$$\psi_i^e = [C_{i3}J_n(k_r^i r) + C_{i4}N_n(k_r^i r)]\sin(n\phi)e^{-k_z z} \dots \quad (37)$$

For instance, we set a continuity equation from  $(i-1)$ th to  $i$ th dielectric layer  $E_{phi}^{i-1} = E_{phi}^i$  (and idem for  $H_\phi, E_z$ ), each equation including the sum  $E^e + E^m$ .

$$\left[\frac{1}{j\omega\epsilon_{i-1}r_{i-1}} * -nk_z\psi_{i-1}^m \sin(n\phi) + (k_r)_{i-1}\partial_r\psi_{i-1}^e \sin(n\phi)\right] - \left[\frac{1}{j\omega\epsilon_i r_i} * -nk_z\psi_i^m \sin(n\phi) + (k_r)_i\partial_r\psi_i^e \sin(n\phi)\right] = 0 \quad (38)$$

We put the following convention :  $r_{i-1} + o(r) \sim r_i - o(r) =$  by definition  $r_{i-1}$ , showing the need to numerate properly the dielectric multi layers. Let name it  $r_i$ , for short. Also that identity is correct  $\forall\phi$ , which may be simplified<sup>28</sup>.

Developing, gives :

$$\begin{aligned} & \left[\frac{1}{j\omega\epsilon_{i-1}r_i} * -nk_z(C_{(i-1)1}J_n((k_r)_{i-1}r_i) + C_{(i-1)2}N_n((k_r)_{i-1}r_i - i)) \right. \\ & \quad \left. + (k_r)_{i-1}(C_{(i-1)3}J'_n((k_r)_{i-1}r_i) + C_{(i-1)4}N'_n((k_r)_{i-1}r_i))\right] \\ & \quad - \left[\frac{1}{j\omega\epsilon_i r_i} * -nk_z(C_{i1}J_n((k_r)_i r_i) + C_{i2}N_n((k_r)_i r_i)) \right. \\ & \quad \left. + (k_r)_i(C_{i3}J'_n((k_r)_i r_i) + C_{i4}N'_n((k_r)_i r_i))\right] = 0 \end{aligned} \quad (39)$$

Such relations drives us to a linear homogeneous system covering the unknown coefficients  $[C]$ , ie we can express it like  $[A][C] = 0$ , where the matrix A is build with continuity equations similar to the precedent one.

## .4 Resolution of the homogeneous system

For a solution to exist, it is necessary that the determinant of A be null. That condition determines the solution in term of  $k_z$ , the value(s) of the longitudinal propagation constant

<sup>27</sup>see part ?? for function names

<sup>28</sup>the false case/paradox  $\phi = 0$  is to be shunted, invoking continuity of the physical solution



of the searched mode. When  $k_z$  is determined, we can deduce  $k_r$  by  $k_r = \sqrt{(k^2 - k_z^2)}$ . Knowing these 2 constants, the computation of the coefficients of scalar potentials, and consequently the components of the electromagnetic fields can be done.

In other side, we have to determine the rank of A, say the dimension of the kernel.

The number of equations Ne is  $4n-2$  :indeed we should have  $4n$  equations of continuity (4 components by layer,  $E_z, E_{phi}, H_z, H_{phi}$ ), but for the first layer, coinciding with the center of the guide, there is no equation. then  $Ne = 4(n - 1) = 4n - 4$ . However, the last layer ends by metallization, it is the frontier of the guide. Then we can write 2 more relations, 1 for E, 1 for H, so  $Ne = 4n - 2$

The number of unknowns Nu is  $4n-2$  :indeed there are 4 coefficients by layer, then  $4n$ , but for the first layer, when  $r \rightarrow 0$ , the function Nn(r) diverge, so it imposes  $C_{12} = C_{24} = 0$ . Finally,  $Nu = Ne = 4n - 2$ .

But  $rank(A)$  is not maximal, then we should have  $rank(A) < dim(A)$  where the inequality is strict ; it is clear that any homogeneous linear system, even with  $detA = 0$ , may have a kernel included into the total initial space. The main point here, is that [26] explain « in general with  $n = 4q - 2$ , the rank of A is  $n-1$  ». To my point it is the weak aspect of the method. Evidently, it must occur cases when a solution doesn't exist ( $rank(A) = 0$ , and no value of  $k_z$ ) or several solutions are coexisting ( $rank(A) < (n - 1)$  strictly, and several values of  $k_z$ ), but isn't it reflecting the physical view? Indeed, « no solution » does not imply no existence of any electromagnetic phenomenon, and multiple solutions expresses probably several scenarii, a mode degeneracy, or coexistence of fairly distinct types of electromagnetic modes.

Anyhow, it is considered, particularly for 2 dielectric layers, that the case  $rank(A) = n - 1$  is statistically major, we shall admit it.

If that question is left aside, considering  $rank(A) = n - 1$  drives us to fix the value of 1 of  $n$  coefficients. Traditionally the first one,  $C_{11} = 1$  for energy normalisation considerations, which can be shown [26]

Consequently, it may be verified that the original matrix can be « cut » by the following procedure : take away the first line ( $rank(A)=n-1$ ), and take away the first column ( $C_{11} = 1$  implies that no left  $n-1$  equations , need first column), and report the first column of  $A_{22} \dots A_{2n}$  in the second member.

Explicitly we have to solve :

$$\begin{pmatrix} A_{22} & \dots & A_{2n} \\ \dots & \dots & \dots \\ \dots & \dots & \dots \\ \dots & \dots & \dots \\ \dots & \dots & \dots \\ A_{2n} & \dots & A_{nn} \end{pmatrix} \begin{pmatrix} C_{21} \\ C_{23} \\ C_{31} \\ C_{32} \\ \dots \\ C_{nn} \end{pmatrix} = - \begin{pmatrix} A_{21} \\ A_{31} \\ \dots \\ \dots \\ A_{n1} \end{pmatrix} \quad (40)$$

Which can be done by LU decomposition and after it, by backward substitution.

## Références

- [1] Abramowitz and Stegun. *Handbook of mathematical functions with formulas, graphs, and mathematical tables*. John Wiley & Sons, Inc, 1972.
- [2] Brogitte Cros and Patric Muggli. Adendum input for the 2020 update of the european strategy for particle, 2020.
- [3] H. Hahn. Deflecting mode in circular irisloaded waveguides. *THE REVIEW OF SCIENTIFIC INSTRUMENTS, VOLUME 34. NUMBER 10*, june 1963.
- [4] Roger F. Harrington. *Time harmonic electromagnetic fields*. McGraw-Hill, 1961.
- [5] S.A.R. Horsley. Indifferent electromagnetic modes : bound states and topology, april 2019.
- [6] Jonathan Hu. Understanding leaky modes : slab waveguide revisited. *Advances in Optics and Photonics 1, 58–106 (2009) doi :10.1364/AOP.1.000058*, January 2009.
- [7] John David Jackson. *Classical Electrodynamics, Third edition*. John Wiley & Sons, Inc, 1998.
- [8] K JuliaLang. Julia 1.4 documentation. <https://docs.julialang.org/en/v1/>, 2020.
- [9] Achint Kapoor and G.S. Singh. Mode classification in cylindrical dielectric waveguides. *JOURNAL OF LIGHTWAVE TECHNOLOGY, VOL. 18, NO. 5*, May 2000.
- [10] S. Krohns, P. Lunkenheimer, Ch. Kant, A. V. Pronin, H. B. Brom, A. A. Nugroho, M. Diantoro, and A. Loidl. Colossal dielectric constant up to gigahertz at room temperature. *Applied Physics Letters*, 94(12) :122903, March 2009.
- [11] Thorsten Liebig. openems - open electromagnetic field solver. <https://www.openEMS.de>.
- [12] Adolphe Vincent Msrtik. *The resolution of the thermodynamic paradox and the theory of guided wave propagation in anisotropic media*. PhD thesis, may 1968.
- [13] Nist. Nist digital library of mathematical functions. url=<https://dlmf.nist.gov/>, 2020.
- [14] Shamini Pillay and Al. Weakly guiding fibers and lp modes in circular and elliptical waveguides. *Journal of Electromagnetic Analysis and Applications*, July 2013.
- [15] William H. Press and al. *Numerical Recipes in C*. CAMBRIDGE UNIVERSITY PRESS, 2002.
- [16] Monireh Ranjbar and Ali Bahari. Investigation of hybrid mode in cylindrical non linear waveguide. *Optik, Volume 157, March 2018, Pages 906-913*, march 2018.

- [17] A. Safaai-Jazi and Al. Classification of hybrid modes in cylindrical dielectric optical waveguide. *Radio Science, Volume 12, Number 4, pages 603-609*, July-August 1977.
- [18] Bernard Schutz. *Geometrical methods of mathematical physics*. Cambridge University Press, 1982.
- [19] H. Seidel. The character of waveguide modes in gyromagnetic media. *THE BELL SYSTEM TECHNICAL JOURNAL*, March 1957.
- [20] D M Shyroki and Al. Dielectric multilayer waveguides for te and tm mode matching. *J. Opt. A : Pure Appl. Opt. 5 (2003) 192-198*, July 2003.
- [21] Jan Skowron and Andrew Gould. General complex polynomial root solver and its further optimization for binary microlenses. May 2012.
- [22] William R. Smythe. *Static and Dynamic Electricity, second edition, p 517*. McGraw-Hill Book Company Inc, July 1950.
- [23] J.A. Stratton. *Electromagnetic Theory*. McGrawHill Book Company Inc, 1941.
- [24] Xiaoli Tang and Al. Elliptical metallic hollow fiber inner-coated with non-uniform dielectric layer. *Vol. 23, No. 17 DOI :10.1364/OE.23.022587 OPTICS EXPRESS 22587*, August 2015.
- [25] Vladimir R. Tuz and Al. Dispersion peculiarities of hybrid modes in a circular waveguide filled by a composite gyroelectromagnetic medium, February 2017.
- [26] K.W. Whites. Electromagnetic wave propagation through circular waveguides containing radially inhomogeneous lossy media. Master's thesis, September 1989.
- [27] Xinyuan Wu. Improved muller method and bisection method with,global and asymptotic superlinear convergence of both point and interval for solving nonlinear equations. *Applied Mathematics and Computation*, 166 :299-311, 07 2005.